3942 - A164
Objective Refraction From the Gradient and Curvature of the Wavefront

R. Navarro. ICMA, CSIC and Universidad de Zaragoza, Zaragoza, Spain.

Purpose: The problem of measuring the objective refractive error of an eye with an aberrometer has shown to be elusive. The purpose of this work is to develop a theoretical framework to determine the refractive error directly from the first and second derivatives of the wavefront.
Methods: In a previous work [Navarro, J. Biomed. Opt. 14, 024021, 2009] the vergence error of a ray, passing through a given point (x, y) at the pupil, and intercepting the retina at another point (X',Y'), was formulated as a 2x2 symmetric matrix: The matrix elements are the ratios between image and pupil coordinates (X'/x, Y'/y, etc.) X' and Y' are partial derivatives of the wavefront. Here an equivalent but more robust formulation is presented in terms of wavefront curvature. Curvature can be approximated by the second fundamental quadratic form of differential geometry. This form is another 2x2 symmetric matrix whose elements are proportional to the second derivatives of the wavefront. For both magnitudes vergence and curvature, the 2x2 matrix represents an infinitesimal elliptical wavefront (around each ray) characterized by a refractive error (sphere, cylinder and axis.)
Results: Vergence error and curvature provide quite similar measures of refractive error of a ray (or infinitesimal patch of a wavefront), but vergence error has singularities at the x and y axes, whereas curvature is well defined at any point inside the pupil. These magnitudes show interesting invariant properties against odd-symmetric aberrations, both for the chief ray and for the pupil average. In particular, wavefront curvature of the chief ray provides the refractive error of the paraxial image. A refractive correction producing a nearly maximum contrast (Strehl ratio) is obtained by cancelling either vergence or curvature for the highest number of rays.
Conclusions: The proposed formulation of refractive error as a 2x2 matrix permits a direct link with both differential geometry of the wavefront (curvature) and geometrical optics (vergence error). One can choose different possible corrections and make approximated estimations of image quality and contrast.
CR: R. Navarro, None.
Support: CICYT (Spain) Grant FIS2008-00697

3943 - A165
Adaptive Optics Asymmetric Double Pass Method to Assess the Ocular Point Spread Function

A. Alarcon[1], *R. Sabesan*[2A], *G. Yoon*[2B]. [1]Department of Optics, University of Granada, Granada, Spain; [A]Institute of Optics, [B]Flaum Eye Institute, [2]University of Rochester, Rochester, NY.

Purpose: The conventional asymmetric double pass with a small entrance pupil (EnP) and a large exit pupil (ExP) is unable to capture higher spatial frequencies in the ocular point-spread-function (PSF) due to an extended laser beacon on the retina induced by diffraction. The goal of this study is to assess the ocular PSF by using adaptive optics (AO) in an asymmetric double-pass with a large EnP.
Methods: Aberrations of light going into the eye (the first pass) for a 6 mm EnP were corrected to produce a nearly diffraction-limited laser beacon at the retina. In the second pass, the reflected light from the retina was imaged through a 6 mm ExP onto a CCD camera to provide an estimate of the PSF. This method was compared to the conventional asymmetric double pass with unequal EnP (1 mm) and Exp (6 mm) and symmetric (EnP and ExP = 6 mm) double pass method. Three model eyes were simulated with varying magnitudes of aberration using phase plates. The PSFs were also obtained in 2 young normal eyes. The measured single pass PSF was used as a reference to assess imaging performance with each double pass technique in the model eye. The cross-correlation coefficients and area under the MTF (aMTF) were computed for comparison.
Results: Two model eyes were dominated by Zernike coma of 2 µm and 0.5 µm respectively while the third model eye mimicked the aberrations of a real normal eye with 0.55 µm in total RMS, all over a 6 mm pupil. Cross-correlation coefficients of the conventional asymmetric and the AO asymmetric double PSFs with the single pass PSF were 0.87 ± 0.03 and 0.78 ± 0.01 on average for the model eyes. The aMTF up to 60 cyc/deg estimated from the single pass PSF, the symmetric and the AO asymmetric double pass were 9.9 ± 2.4, 14.2 ± 5.2 and 7.6 ± 2.9 respectively. Beyond the spatial bandwidth of the conventional asymmetric method, the AO asymmetric double pass also increases the aMTF by an average factor of 5.24 and 2.14 in model eyes and real eyes respectively.
Conclusions: AO asymmetric double pass provides a reliable estimate of the ocular PSF directly and has the potential to detect the optical defects that can not be detected by an ocular wavefront sensor. The ability to measure the PSF reliably facilitates an assessment of the ocular optical transfer function.
CR: A. Alarcon, None; **R. Sabesan**, None; **G. Yoon**, Bausch and Lomb, F.
Support: Junta de Andalucia Spain P07-FQM-02663, NIH/NEI 5R01EY014999, NYSTAR/CEIS,RPB

3944 - A166
A New Method for Characterization of Transverse Chromic Aberration of Ophthalmic Lens

G. Li. College of Optometry, University of Missouri - St. Louis, St. Louis, MO.

Purpose: Transverse chromatic aberration causes lateral smearing or blurring of the images on retina due to color dependent magnification, and it is an important performance parameter for ophthalmic lens. The transverse chromatic aberration is usually characterized by the prism diopters and the Abbe number of the lens material, which involves the refractive indices at wavelengths 589.3 nm, 486.1 nm and 656.3 nm, and the latter two wavelengths are away from the photopic peak. Here a new parameter, called effective Abbe number is introduced and used to characterize the transverse chromatic aberration.
Methods: The measurement is performed at 543 nm and 594 nm, which are close to the photopic peak and available with commercial tunable He-Ne laser. A computer-interfaced optical setup has been built for this test. It requires only the laser beam displacements due to the angular deviation imparted by the lens. Other parameters such as the lens power, the distance of the measurement location from the center of the lens, and the distance from the lens to the camera are not required.
Results: Composite lenses with -2D, -4D, -6D powers made with two singlets and a photosensitive layer in between to increase the effective Abbe value at radii away from the optical center have been tested. The effective Abbe value measured in the periphery of the lens was increased from a nominal base plastic value of 42.0 to a value of 46.0. The increase in visual acuity due to increases in effective Abbe value can be accurately estimated based upon measured vision data in the published literature.
Conclusions: The effective Abbe number gives a much better indication of visual performance than the actual Abbe number. Using this method, experimental results for the electro-optic ophthalmic lens will be reported.
CR: G. Li, None.
Support: National Institutes of Health grant 1R21EB008857, The Wallace H. Coulter Foundation Career Award grant WCF0086TN, and University of Missouri Research Board.

3945 - A167
Interferometric Lens Meter for the Testing of Local Second and Higher Order Aberrations of Progressive Addition Lenses

E. Acosta[1], *S. Chamadoira*[1], *R. Blendowske*[2]. [1]Applied Physics, Univ of Santiago de Compostela, Santiago de Compostela, Spain; [2]Optical Technologies and Image Processing, Hochschule Darmstadt, Darmstadt, Germany.

Purpose: To develop a simple experimental set-up to determine the local aberrations of progressive addition lenses. Aberration variation resulting from increased patch size around the measurement is also included. In the case of small patches, where higher order aberrations are negligible, the set-up provides the local dioptric power matrix (sphere and astigmatism) of the lens.
Methods: The experimental set-up is basically a point diffraction interferometer which has been modified in order to provide fringe patterns within small areas of the lens (patch diameters ranging from 1 to 5 mm). The lens remains in a fixed position and only one part of the set-up needs to be translated along one axis (approximately 20 mm), acting like a Badal system to compensate for defocus, and on the perpendicular plane (approximately 3 mm) to compensate for prismatic effects. Additionally, the region under test is selected in accordance with this movement.
Results: The calibration of the most simple version of the set-up shows that local sphere and astigmatism are determined with less than 0.1 D accuracy. Higher order aberrations are determined with an accuracy of about one tenth of a wavelength. In this first version, the inspection area is within a circle measuring approximately 25 mm in diameter. No compensating optics are used to correct the sphere and no rotatable elements or compensating prisms are used to choose the region of interest or to scan the lens. Range of measurement is -10 D to 10 D for additions up to 2.5 D. And lastly, it is worth pointing out that the number of measurement zones can be selected based on user criteria (from a single zone up to a complete scan in increments of 1 mm in both directions). In any case, the diameter of the region of interest around the point can also be chosen.
Conclusions: We have developed a compact and robust interferometric lens meter capable of providing both the map of local sphere and astigmatism as well as aberrations for different pupil sizes. This will help to predict quality of vision through the different zones of progressive addition lenses.
CR: E. Acosta, None; **S. Chamadoira**, None; **R. Blendowske**, None.
Support: Ministerio de Educación y Ciencia, Spain (grants nº FIS2007-63123) and Xunta de Galicia, INCITE09E1R206060ES

3946 - A168
Developing an Adaptive Phoropter Through the Application of a Fluidic Lens and Shack Hartmann Sensor

N. Savidis[1A], R. Marks[1A], N. Peyghambarian[1A], D. Mathine[1A], G. Peyman[1A], J. Schwiegerling[1B]. [A]Optical Sciences, [B]Ophthalmology, [1]University of Arizona, Tucson, AZ.

Purpose: Develop an adaptive phoropter that automatically measures spherical and cylindrical error and nulls this error with a sphero-cylindrical fluidic lens.
Methods: An automated phoropter has been designed and fabricated. The system is comprised of three modules: a fluidic lens, a relay telescope and a Shack-Hartmann sensor. The fluidic lens is a stack of three adjustable lenses composed of a spherical lens and two astigmatic lenses oriented 45 degrees to one another. Any sphere, cylinder and axis combination can be achieved by adjusting the fluid volume within the fluidic lenses. Following the fluidic lens, are a relay telescope and a beamsplitter. The beamsplitter directs infrared light towards the final module: a Shack-Hartmann wavefront sensor. The beamsplitter also passes visible light, allowing for the subject to view external targets such as an eye chart. The system works as follows. (1) Infrared light is shone into the eye and scatters from the retina. (2) The scattered light exits the eye as an emerging wavefront that is relayed through the fluidic lens to the Shack-Hartmann sensor. The sensor reconstructs the wavefront and extracts the sphero-cylindrical refractive error. This prescription is then applied to adjust the volume of the fluidic lenses in an attempt to null out the refractive error. Feedback of the wavefront from the eye/fluidic lens combination is then used to monitor the fluid volume and keep the net refractive error at a minimum. A raytracing model has been developed to determine the properties and ranges of the automated phoropter.
Results: The raytracing model shows that the Shack Hartmann sensor is capable of measuring a spherical refractive error from -25 to 40 D. Even in cases of extreme myopia or hyperopia, a limited number of spots are needed to drive the fluidic lens power in an appropriate direction, forcing the Shack-Hartmann pattern into a more useable range.
Conclusions: Fluidic lenses coupled with a Shack-Hartmann sensor applied in an eye examination have the potential of creating an automated means of measuring and nulling a subject's prescription. The goal is to produce a reliable device that allows for quick and inexpensive objective measurement of a subject's prescription.
CR: N. Savidis, None; **R. Marks**, None; **N. Peyghambarian**, None; **D. Mathine**, None; **G. Peyman**, None; **J. Schwiegerling**, None.
Support: NIH Grant EY018934A

3947 - A169
Measuring Light Scatter With a Shack-Hartmann Wavefront Aberrometer

J. Nam, N.L. Himebaugh, H. Liu, L.N. Thibos. School of Optometry, Indiana University, Bloomington, IN.

Purpose: To develop a quantitative method for specifying the amount of light scatter at different locations in the eye's pupil. A spatially-resolved measure of light scatter may be useful for studies of tear film, cataract, corneal transparency, and refractive surgery.
Method: We assume the mechanism of light scatter by the eye can be modeled as a random phase screen (Goodman, *Statistical optics*, 2000). Invoking reasonable simplifying assumptions, the point-spread function (PSF) of a single lenslet in a Shack-Hartmann wavefront aberrometer (SHWA) is the convolution of two other PSFs. First is the PSF due to ocular wavefront aberrations over a sub-aperture defined by the lenslet face, and second is the PSF due to light scattered by that portion of the random phase screen associated with the lenslet. This convolution relationship enables a simple rule: the size of the lenslet's PSF is the sum of the size of the PSF due to wavefront aberrations and the size of the PSF due to scatter. We define "size" in this context as the radial variance of the light distribution in the PSF. Applying this rule twice to account for the double-pass nature of the SHWA enables an accounting of the amount of blur on each pass. The method was validated on a theoretical test case and feasibility was assessed with a human eye before and after tear breakup. The theoretical model subtracted a Gaussian function C*exp(-R/2S) from the wavefront error map, where R is the squared radius of points over the lenslet aperture relative to the lenslet center.
Results: For a range of parameter values (-1<C<2 microns; $\sqrt{S} < 3$*lenslet diameter), the measured size of the double-pass image produced by each lenslet agreed with expected values with less than 2% error. Measurements on a human eye before and after substantial breakup of the tear film were feasible and indicated a significant, measurable increase of SHWA spot size due to light scatter.
Conclusion: Spatially-resolved measurements of light scatter using a SWHA is a valid procedure that is feasible for quantifying the light-scattering effects of tear film breakup.
CR: J. Nam, None; **N.L. Himebaugh**, None; **H. Liu**, None; **L.N. Thibos**, None.
Support: NIH Grant R01-EY05109

3948 - A170
Clinical Validation of a Modified Wavefront Analyzer - Preliminary Results

B.-U. Seifert[1], S. Schramm[1], P. Bessler[1], P. Schikowski[2], K.S. Kunert[3]. [1]Biomedical Engineering and Informatics, Ilmenau University of Technology, Ilmenau, Germany; [2]GMC Systems, Ilmenau, Germany; [3]Dept. of Ophthalmology, Helios Klinikum Erfurt, Erfurt, Germany.

Purpose: To quantify the influence of modifications made to a commercially available wavefront analyzer (WASCA, CZM AG). Modifications aim for combined measurements of aberrations and scatter of the eye using one integrated device based on Hartmann-Shack technology. To increase the amount of straylight imaged onto the sensor a confocal pinhole, typically used to suppress corneal reflections and to improve spot imaging, has to be extended. To reduce effects of corneal reflections the instrument is adjusted off-axis. Both pinhole extension and off-axis adjustment hold the capability of altering the aberration measurements which has to be investigated.
Methods: Two similar wavefront analyzing devices (WAD) where introduced. WAD1 featured the original confocal pinhole whereas pinhole of WAD2 was extended to 8 mm in diameter. To suppress corneal reflections the optical axis of the device was shifted to the temporal side. Measurements where performed on 5 subjects (36.2+/-8.1 years, -1.10+/-1.55 dpt) on both eyes. Each eye underwent the following measurement modes: WAD2 off-axis, WAD1 off-axis, WAD1 on-axis yielding 10 samples per eye and per mode. Zernike coefficients up to 4th order where analyzed. Samples where tested for normal distribution ($p<0.05$). T-Test and f-Test were performed to assess comparability and reproducibility regarding different pinhole size and axis shift.
Results: Temporal shift of the device axis resulted in a significant difference of 4 Zernike coefficients in total ($p<0.05$, left: 3, right: 1). Temporal shift in conjunction with an extended pinhole further increased it to a total of 10 Zernike coefficients of significant difference ($p<0.05$, left: 7, right: 3). F-test across the measurement modes showed no significant difference in standard deviation.
Discussion: Despite the limited number of subjects there is at least some evidence that modifications intended for scatter measurement in the eye by conventional wavefront analyzer affect the aberration measurement characteristics. It can be concluded that for simultaneous assessment of aberration and scatter within one single device a sequential procedure is advisable to ensure optimum conditions for each mode. A currently on-going study will help to overcome limitations due to population distribution and size.
CR: B.-U. Seifert, None; **S. Schramm**, None; **P. Bessler**, None; **P. Schikowski**, GMC, E; **K.S. Kunert**, None.
Support: Granted by TAB 2008 FE 9093

3949 - A171
Reproducibility of Straylight Measurement by C-Quant for Assessment of Retinal Straylight With the Compensation Comparison Method

G.I. Guber[1], T.M. Thiel[2]. [1]Eye clinic lucerne, Eye clinic lucerne, Lucerne, Switzerland; [2]Eye Clinic Lucerne, Eye Clinic Lucerne, Lucerne, Switzerland.

Purpose: Disability glare gives the appearance of a veil of light thrown over a person's vision when there is a strong light source present. It is generally accepted that this glare is caused by imperfections in the optical media causing a non-uniform passage of light on its way from its source to the subject's retina. Because the glare is caused by light incident to the retina, this is termed forward light scatter. Conversely, back scatter is dispersion of light reflected out of the eye and can be seen by an external observer. The C-Quant is a new device for subjective measurement of forward straylight. We examined the reproducibility of the measurements in dependence of the refraction, eye pigmentation and patient's age.
Methods: We performed on the subject's dominant eye 5 repeated-measures after refraction was determined. The measurement is based on the "compensation comparison" method whereby the subject's task is a forced-choice comparison between two half fields (one with and one without counterphase compensation light), to decide which half flickers more strongly.
Results: 41 healthy subjects, age of 21 to 59y (mean 37,5y) were examined (14 emmetropic, 16 myopic, 7 hyperopic and 4 with astigmatism; 18 with bright and 23 subject with dark eyes). The mean investigation duration of all measurements was 1.37s whereby the duration shortened of initially 1.53s to 1.32s. There was no significant difference between the different groups of refraction, but subjects with bright eyes had significantly higher straylight values.
Conclusions: The importance of testing disability glare in ophthalmic patients is increasing as surgical technology and patient expectations advance. C-Quant is suited for quick and reproducible measurement in patients with complaints caused by straylight.

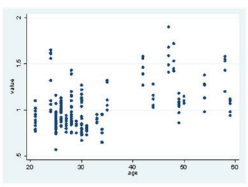

The graph shows the distribution of straylightparameters in relation to the age

CR: G.I. Guber, None; **T.M. Thiel**, None.
Support: None

3950 - A172
On and Off-Axis Ocular Length Measurements Using the IOLMaster

S.M. Delgado[1,2], D. Falk[1,2], K. Ehrmann[1,2], A. Ho[1,3], P. Sankaridurg[1,2]. [1]Institute for Eye Research, Sydney, Australia; [2]Vision Cooperative Research Centre, Sydney, Australia; [3]School of Optometry & VIsion Science, University of New South Wales, Sydney, Australia.

Purpose: Measure on and off-axis ocular length using the IOLMaster (Carl Zeiss Meditec AG, Germany) while maintaining an open-field of view.
Methods: An IOLMaster was modified to allow for presentation of real-space fixation targets. Five subjects (aged 25-29 years) were assessed in a feasibility study using the modified set-up. Only the left eyes (OS) were measured; OS spherical equivalent refractive errors (RE) ranged from -4.81D to +0.06D with cylinder <1.00D. The axial length (AL) was determined for all subjects during a) distance vision under dilated conditions using 1% tropicamide and b) while subjects fixated on a 5D accommodative demand near target. Off-axis dimensions were measured at 5°, 10°, 20°, 25° and 30° in the nasal and temporal visual fields under dilated conditions. Measurements were repeated until at least 3 values with a signal-to-noise ratio (SNR) of ≥2.0 and standard deviation ≤0.03 mm were realized.
Results: The accuracy and precision of the modified set-up was assessed for on-axis conditions using the IOLMaster calibration eye (labelled AL of 20.77±0.05 mm versus measured AL of 20.79±0.01 mm using either the standard or modified set-up). The standard and modified set-up yielded respective SNR values of >37.0 and >11.0. The change in measured AL during accommodation was 0.00±0.04 mm for 5 eyes. The graph shows the results for on and off-axis length for 3 eyes that achieved the SNR criteria for off-axis measurements, and includes a calculation for a schematic eye, all with tilt and asymmetry data.
Conclusions: It is feasible to measure on and off-axis ocular length using an open-field IOLMaster; this method provides a non-invasive option for measuring eye contour during fixation on real-space targets. Our results do not account for the possible change in the eye's group refractive index as a function of off-axis fixation angle or accommodation. A correction factor is being investigated.

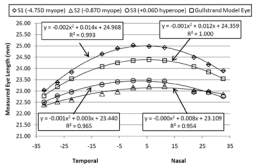

CR: S.M. Delgado, None; **D. Falk**, None; **K. Ehrmann**, None; **A. Ho**, None; **P. Sankaridurg**, None.
Support: Funded by grants from the Institute for Eye Research, the Australian Government CRC Scheme through the Vision CRC and the Whitaker International Fellowship (Delgado).

3951 - A173
Ocular Aberrations in the Peripheral Visual Field With a Commercial Open-View Aberrometer

K. Baskaran, B. Theagarayan, S. Carius, J. Gustafsson. School of Optometry, Linnaeus University, Kalmar, Sweden.

Purpose: The interest in off-axis aberrations has increased with the discovery of a possible link between myopia development and peripheral optics. The most common technology to measure the off-axis aberrations is a Shack-Hartmann wavefront aberrometer. This is the first study to report peripheral aberrations in a large sample of emmetropic population with a commercial open-view Shack-Hartmann aberrometer.
Methods: The commercial open-view Shack-Hartmann aberrometer COAS-HD VR was used to measure the aberrations in the peripheral vision. Aberrations of the right eye of 30 emmetropes (24 ± 4 years) were studied. Off-axis aberrations were measured in steps of 10° out to ± 30° in the horizontal visual field. The subjects turned their eye to view the off-axis fixation target (light emitting diode placed at 3 meters) during the measurement. The resulting wavefront aberrations were parameterized with Zernike coefficients for a 5 mm diameter pupil. All analyzes are reported according to optical society of America (OSA) recommended standards.
Results: Aberrations from the 2nd to 6th order and the total higher-order root-mean-square (HO RMS) were analyzed using one-way ANOVA. The defocus C^0_2 was significantly myopic in the nasal visual field (+20°, +30°) whereas there was no significant difference in the temporal visual field. Astigmatism C^2_2 increased quadratically from ±10° in the periphery and coma C^1_3 showed a linear increase across the horizontal visual field ($p < 0.05$). The spherical aberration C^0_4 and the total HO RMS showed a significant change at ±30°.
Conclusions: Our results showed that in young emmetropes there was a significant increase of HO RMS at ±30°, which is expected. Astigmatism, horizontal coma, and spherical aberration vary systematically across the horizontal visual field in agreement with Seidel theory. The findings of our study with a large sample of emmetropic population agree with the previous studies done with laboratory built aberrometers.
CR: K. Baskaran, None; **B. Theagarayan**, None; **S. Carius**, None; **J. Gustafsson**, None.
Support: This research was supported by the Faculty of Natural Sciences and Technology, University of Kalmar and the foundation Sparbanksstiftelsen Kronan.

3952 - A174
A New Approach for the Study of the Spatial Statistics of the Eye Aberration

E. Pailos[1], A. Ommani[2], L. Diaz-Santana[2], S. Bará[1]. [1]Fisica Aplicada (Area de Optica), Universidade de Santiago de Compostela, Santiago de Compostela, Galicia, Spain; [2]Henry Wellcome Laboratories for Vision Science, Department of Optometry and Visual Science, City University, London, United Kingdom.

Purpose: We present a new method to characterize the spatial statistics of the ocular aberrations and show how to apply it to a sample of healthy eyes. In particular, we assess the compatibility of simple eye aberration statistical models with the experimental centroid displacements provided by a Hartmann-Shack wavefront sensor (HS).
Methods: Initial information about the aberrations statistics is obtained from the centroid diagrams (defined as the plot of the positions of the centroids of the HS lenslet array for all the series measured for a given eye). We then compute the theoretical values of the second-order statistical functions of the sensor centroid displacements for two statistical models of aberration statistics: (1) defocus driven, and (2) power-law (Kolmogorov-like). Using a chi-square test, we check the compatibility of these predictions with the estimates of the same magnitudes from the experimental centroids: Two sets of uncorrected eyes under normal accommodation conditions were used: (a) 41 eyes from a middle-aged group (45 to 65 years) of 21 people and (b) 12 eyes from 6 people below 45 years. HS data were collected at 24 Hz using a laser diode at 780 nm.
Results: The eyes of the young-aged group that had a strong defocus fluctuation showed a characteristic inhomogeneous behavior, as their centroid diagrams and the plots of their centroid variances revealed. This is incompatible with the homogeneity of power-law models. The chi-square test performed for the centroid displacements structure function also dismissed power-laws (at a 5% significance level). For those eyes with weaker defocus fluctuation, the high variability of the data made this latter test not significant for both defocus and power-laws. The statistics observed for the middle-aged group showed a higher degree of homogeneity and isotropy; power-law models could not be ruled out as candidates for the description of these eyes.
Conclusions: The method presented skips the aberrations estimation stage and works with HS measurements instead. This procedure simplifies the comparison of results between labs (the specification of the reconstruction parameters is not needed) and avoids any loss of information due to the estimation step. The results obtained stress the importance of the defocus fluctuations in young eyes. Forthcoming models of the individual eye aberrations must take into account the high weight of this term in relation to that contained in power-law models.
CR: E. Pailos, None; **A. Ommani**, None; **L. Diaz-Santana**, None; **S. Bará**, None.
Support: MICINN grant FIS2008-03884; EPSRC grant GR/S58812/01(P); USWR.AS.IR grant (AO); MEC FPU grant AP2004-0122 (EP).

3953 - A175
To Study the Modulation Transfer Functions of the Total Visual Perception, the Optical, and the Neurophysiologic Systems According to Wavefront Analysis

M. Fukui[1], T. Mizutani[1], K. Yatsui[1], H. Kubono[1], Y. Kitada[1], H. Tanaka[1], R. Fukushima[1], K. Ohnuma[2], T. Noda[1]. [1]National Hospital Organization Tokyo Medical Center, Tokyo, Japan; [2]Med System Course/Grad Sch of Eng, Chiba University, Chiba-shi, Japan.

Purpose: To study the modulation transfer functions (MTFs) of the total visual perception, the optical, and the neurophysiologic systems using wavefront analysis.
Methods: Ten eyes of five healthy individuals (average age, 29.6 ± 2.6 years) without cataract were tested. The contrast visual acuities using the Landolt ring charts of various sizes and contrasts were measured and the contrast sensitivity function of the total visual perception system was obtained. The wavefront aberrations were measured using a wavefront analyzer (KR-1W, Topcon), and the MTF of the ocular optical system was obtained. According to wavefront analysis, simulated images, in which the Landolt rings with contrast values of recognition-threshold levels were projected on the retina, were synthesized using optical simulation software (Retinage™), and the contrast values at the break in the simulated Landolt ring image (i.e., neurophysiologic contrast sensitivity) were calculated. The MTFs of the total visual perception, the optical, and the neurophysiologic systems were compared.
Results: The mean threshold contrast sensitivity values in the total visual perception/neurophysiologic systems were 74%/6.0% at logMAR (-0.1), 27%/4.1% at logMAR (0), 14%/2.5% at logMAR (0.1), 6.0%/1.4% at logMAR (0.2), 4.0%/0.8% at logMAR (0.3), and 3.0%/0.48% at logMAR (0.4), respectively. Decreased contrast images projected on the retina through the optical system seemed to be enhanced by neurophysiologic functions depending on the image size.
Conclusions: These data provide a useful basic physiologic background on the vision tests using Landolt rings. Wavefront analysis combined with an accumulated clinical database of normal values of neurophysiologic contrast sensitivity may be useful in differential diagnosis between optical and neurophysiologic functions in cases with visual disturbances.

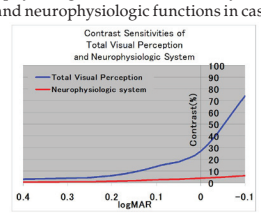

CR: M. Fukui, None; **T. Mizutani**, None; **K. Yatsui**, None; **H. Kubono**, None; **Y. Kitada**, None; **H. Tanaka**, None; **R. Fukushima**, None; **K. Ohnuma**, None; **T. Noda**, None.
Support: None

3954 - A176
The Impact of Individual Zernike Coefficients on Retinal Image Quality

J. Buehren, T. Kohnen. Dept. of Ophthalmology, Goethe University Frankfurt am Main, Frankfurt am Main, Germany.

Purpose: To compare the impact of individual Zernike coefficients on retinal image quality in normal eyes using a simulation experiment.
Methods: Wavefront errors of 500 normal eyes (274 subjects) were reconstructed with Zernike polynomials (2nd-5th order) over a pupil diameter of 6 mm. Distance correction was simulated using a lower-order aberrations (LOA) optimization algorithm based on the VSOTF metric (visual Strehl ratio of the optical transfer function) to minimize the influence of LOA. An ideal, diffraction-limited wavefront served as control. Each coefficient was modified separately from -1 µm to 1 µm in 0.1 µm steps while all other Zernike coefficients were kept constant and the VSOTF metric was calculated from each modified wavefront error. Tolerance to aberration-induced deterioration of retinal image quality was defined as the range over which the VSOTF did not decrease more than 0.2 log units from its maximum value.
Results: In the diffraction-limited eye, tolerances ranged from <0.1 µm ($C_5^{\pm1}$) to 0.4 µm ($C_2^{\pm2}$). In real eyes, tolerance values varied between 0.24 µm (C_5^{-1}) and 1.52 µm (C_5^{-5}) with lowest tolerances for the coefficients at the center of the Zernike pyramid. Improvement of retinal image quality with coefficient values different from zero could be observed with C_2^0 (maximum VSOTF at 0.5 µm), C_3^{-1} (-0.1 µm) and C_4^0 (0.1 µm).
Conclusions: (1) In eyes with physiological aberrations, the impact of individual Zernike coefficients on retinal image quality was not equal. (2) The presence of physiological higher-order aberrations decreased retinal image quality but mitigated the impact of individual coefficients on image deterioration.
CR: J. Buehren, None; **T. Kohnen**, None.
Support: None

3955 - A177
Impact of Positive and Negative Defocus on Visual Acuity

B. Vasudevan, IV[1A], A. Bradley[1A], L.N. Thibos[1B], J. Martin[1C], J. Nam[1A], N.L. Himebaugh[1C]. [A]Vision Science, [B]Optometry, [C]School of Optometry, [1]Indiana University, Bloomington, IN.

Purpose: Because of the profound differences in the retinal images generated by positive and defocused in an aberrated eye, we examined the visual impact of both types of defocus.
Methods: Twenty subject eyes participated in the study. All the subjects were cyclopleged with 1% cyclopentolate in right eye only, and aberrations were measured using COAS at 630nm. Forced choice staircase methods were used to measure letter acuity after subjective refraction. Defocus was controlled by inserting ophthalmic lenses in front of a 3 or 6 mm artificial pupil that was imaged into the eye's pupil plane using a unit magnification telescope. Single letters and 3X3 clusters of letters were presented for 1 second, subjects used a keyboard to identify the (central) letter.
Results: In most eyes, positive defocus produced a fairly linear increase in logMAR (mean slope = 0.5 logMAR/Diopter), but significant non-linear effects contributed to shallower slopes (mean slope = -0.32 logMAR/Diopter) with negative defocus when testing with single letters. Between -1 and -2 diopters, many subjects showed a dramatic decline in the effect of increased negative defocus, and in some cases single letter VA actually improved with increasing defocus. Within this dioptric range, many observers report performing the acuity task by simply reading one of the doubled images observed. Image doubling is consistent with computed images for these eyes based upon measured higher order aberrations and negative defocus. The different impact of positive and negative defocus on acuity was greatly reduced when using the 3X3 letter clusters. With this stimulus, the doubled target images were spatially superimposed with doubled images from the surrounding characters.
Discussion: Our results indicate that, in eyes with positive spherical aberration, negative defocus can generate multiple or double images. This doubling was particularly detrimental to VA when using clusters of characters such as found in text. The loss of visual performance associated with positive and negative defocus may, therefore, be attributed to quite different types of image degradation, and thus the vision loss experienced by myopes and presbyopes/hyperopes is likely to be qualitatively different.
CR: B. Vasudevan, IV, Essilor Corporation, F; **A. Bradley**, Essilor Corporation, F; **L.N. Thibos**, Essilor Corporation, F; **J. Martin**, Essilor Corporation, F; **J. Nam**, Essilor Corporation, F; **N.L. Himebaugh**, Essilor Corporation, F.
Support: Essilor Corporation

3956 - A178
How Many JNDs of Blur Before One Line of Best Corrected VA is Lost?

A. Ravikumar[1A], Y. Shi[1A], H.E. Bedell[1B], R.A. Applegate[1A]. [A]Visual Optics Institue, College of Optometry, [B]College of Optometry, [1]University Of Houston, Houston, TX.

Purpose: In refractive surgery "20/20 happy" vs "20/20 unhappy" is a common clinical criterion to differentiate success and failure. Our purpose was to determine the number of JNDs for blur that corresponds to a one line loss of best corrected VA in a normal eye.
Methods: The 3mm wavefront error (WFE) through the 5th radial order of a well corrected average young eye from the Thibos et al 2002 data set served as the underlying WFE to determine the JND. The coefficients of each Zernike mode were scaled up and down to yield 9 log VSOTF(Visual Strehl ratio computed in frequency domain) values ranging from 0.00 to -0.40 in steps of 0.05 log units. For each of the 9 test conditions, 10 unique letter arrangements of a 100% contrast, three line acuity chart (0.1, 0.0 and -0.1 logMAR) were convolved with PSFs resulting from the scaled WFEs. Three normal subjects had one eye dilated (1% tropicamide) and viewed 300 cd/m^2 test charts at 10 ft through a 3mm pupil with the other eye occluded. Using a temporal forced choice paradigm, subjects compared each test chart to a unique reference test chart (log VSOTF value of -0.20) and indicated which chart was blurrier. The difference between 80% and 50% on the psychometric functions fit to 3 replications defined a JND in log VSOTF for each subject. To determine the change in log VSOTF necessary to induce a one line loss in VA, VA was measured up to the 5th letter miss for a series of logMAR charts constructed as above for log VSOTF between 0 to -1.5 in steps of 0.3 log units. Log VSOTF was linearly regressed against logMAR acuity.
Results: The linear regression revealed a best fit line (y = -3.06x - 0.30), with $R^2 = 0.987$. Consequently, a change of 0.31 in log VSOTF induced a loss of one line of logMAR acuity (e.g., -0.1 to 0.0 logMAR). The average JND was 0.049 ±0.014 log VSOTF. Thus, ~6 JNDs comprise 1 line of log MAR acuity.
Conclusions: Different outcomes within the range of 6 JNDs in log VSOTF that correspond to a line of best corrected acuity provide a plausible explanation for the distinction between "20/20 happy" and "20/20 unhappy".
CR: A. Ravikumar, None; **Y. Shi**, None; **H.E. Bedell**, None; **R.A. Applegate**, None.
Support: NIH/NEI R01 EY08520 (RAA), NIH/NEI R01 EY019105 (RAA), NIH/NEI P30 EY 07551 (Core Grant)

3957 - A179
The Effects of Spherical Aberration on Accommodative Response in Different Refractive Groups

Y. Wu[1], B.-C. Jiang[2]. [1]Ophthalmology, Eye & ENT Hospital of Fudan University, Shanghai, China; [2]Coll of Optometry, Nova Southeastern University, Fort Lauderdale, FL.

Purpose: To compare the effects of spherical aberration on accommodative response between different refractive groups.
Methods: The accommodative responses induced by negative lenses from 0 to -5 D with 1 D step were measured with a COAS device for 10 emmetropes (EMs), 13 stable myopes (SMs), and 9 progressing myopes (PMs). Three types of accommodative response were calculated from each subject's wavefront aberration data with his/her natural pupil size. The total accommodative response (tAR) was based on Zernike defocus term. The paraxial accommodative response (pAR) was based on Zernike defocus and spherical aberrations. In addition, we added the spherical aberration at the edge of 3.5 mm pupil to the pAR and defined it as the AR-3.5. This item was used for simulating the measurement obtained from auto-refractor such as Canon R-1. The difference between pAR and tAR, which was called as apparent defocus shift (ADS), was plotted as a function of accommodative response error of tAR (tAE). Each subject's accommodative stimulus-response curve (ASRC) under tAR, pAR, or AR-3.5 condition was fitted by a regression line. We compared the ASRCs and the ADS/tAE curves between the three groups and within each group.
Results: The slope of ASRC was significantly steeper for pAR than for tAR and AR-3.5 in each group (paired sample test, all $p < 0.05$). Each subject's ASRC data was used to calculate the accommodative error index (AEI, Chauhan & Charman, 1995), which mainly represented the accuracy of accommodative response. The AEI results were not significantly different between tAR, pAR, and AR-3.5 within each group. Under each condition of tAR, pAR, or AR-3.5, the slope of ASRC and the AEI was not significantly different between groups ($p > 0.05$). The relationship between ADS and tAE for each group was linear (EMs: $p = 0.001$; SMs: $p = 0.004$; PMs: $p = 0.001$). The slope of ADS/tAE was significantly shallower in the PMs (0.3477) than in the EMs (0.5564) and SMs (0.6006) (linear regression comparison, all $p < 0.05$).
Conclusions: When we use tAR and AR-3.5 to represent the accommodative response, the spherical aberration of the eye has a significant effect on the slope of ASRC, which is consistent with previous studies. However, our results suggest that the spherical aberration does not change the accuracy of accommodation (AEI). In addition, the effect of spherical aberration on the slope of ASRC is less in the PMs than in the EMs and the SMs.
CR: Y. Wu, None; **B.-C. Jiang**, None.
Support: NSU PFRDG Grant 335441 and NSU HPD Grant 335230

3958 - A180
Determination of the Optimum Weighting of Objective Refractions for Predicting Subjective Refraction

J. Martin[1A], L.N. Thibos[1B], A. Bradley[1C], B. Vasudevan[1C], N.L. Himebaugh[1B]. [A]School of optometry, [B]Optometry, [C]School of Optometry, [1]Indiana University, Bloomington, IN.

Purpose: The purpose of the study was to determine the optimum weighting of the 34 objective refractions for predicting acuity refraction.
Methods: This study was on 20 healthy subjects, cyclopleged with 1 drop of 1% cyclopentolate hydrochloride. In the psychophysical experiments the subject viewed a visual target through an afocal telescope that imaged an artificial pupil (6mm diameter) into the entrance pupil of the eye. Visual acuity was determined with a staircase paradigm for high (96%) contrast letters presented with quasi-monochromatic (635nm) light on a screen placed 2.5 meters from the artificial pupil of the telescope. Subjective refraction is the spherical lens power that maximized acuity. Ocular wavefront aberrations were measured, using a COAS aberrometer (Wavefront Sciences, Inc.) modified to use visible light (635nm). Objective wavefront refraction was performed computationally by determining the additional lens power required to maximize retinal image quality using 34 metrics (Thibos et al, JOV 2004).
Results: Wavefront refractions agreed closely with acuity refractions obtained with 635nm light. A Partial least square (PLS) regression analysis was performed to reduce the number of objective predictors based on their ability to account for the variance in the subjective data. Taken together, the 34 metric-based refractions accounted for 99.26 % of variance in the data. The OTF metric (VNOTF) refraction accounted for about 97.9 of the variance in subjective refraction. Addition of a PSF-based metric-refraction (VSX) enabled the model to account for 98.74% of the variance. Adding a third metric refraction based on wavefront quality (PFWc) accounted for 98.9% of variance in subjective refraction. For this 3-component model, predicted refraction = 0.2094*(refraction based on VNOTF) + 0.1303*(refraction based on VSX) + 0.1167*(refraction based on PFWc).
Conclusion: Subjective refractive errors are accurately and precisely determined by wavefront-based objective refraction in monochromatic light.
CR: J. Martin, Essilor Corporation, F; **L.N. Thibos**, Essilor Corporation, F; **A. Bradley**, Essilor Corporation, F; **B. Vasudevan**, Essilor Corporation, F; **N.L. Himebaugh**, Essilor Corporation, F.
Support: Essilor Corporation

3959 - A181
The Effects of a Convex Mirror on Ocular Accommodative Systems

T. Nagata[1,2], T. Iwasaki[1], A. Tawara[1]. [1]Ophthalmology UOEH, Univ of Occup & Environ Health, Kitakyusyu, Japan; [2]Aso Iizuka Hospital, Iizuka, Japan.

Purpose: Convex mirrors are universally used to see a rear or side area in factories and automobiles. However, the ocular accommodative responses to images observed through a convex mirror have not yet been fully examined. This study investigated the effects of the convex mirror on human ocular accommodative systems.
Methods: Seven young adults with normal visual function were recruited. Each subject was ordered to binocularly watch a target located 2.00 m (0.50 D) from their right eyes through a convex mirror. The steady-state accommodative responses of their right eyes were measured with an infrared optometer for 50 seconds. The measurements were performed twice for each subject. The accommodative responses through a plane mirror were also measured as controls.
Results: The average ocular accommodation of all subjects while viewing through the convex mirror were significantly nearer than through the plane mirror (1.54 D in the convex mirror and 0.39 D in the plane mirror, $p<0.0001$, t-test) although all subjects perceived that the position of the target through the convex mirror was farther away than through the plane mirror. The fluctuations of ocular accommodation were significantly larger while viewing through the convex mirror than through the plane mirror for each subject ($p<0.001$, F-test respectively). Moreover, all of them felt blurred vision and discomfort while viewing through the convex mirrors.
Conclusions: The convex mirror was thought to cause the 'false recognition of distance', which would induce the large accommodative fluctuations and the blurred vision. Caution is necessary when using convex mirrors.
CR: T. Nagata, None; **T. Iwasaki**, None; **A. Tawara**, None.
Support: None

3960 - A182
Wave Aberration of the Mouse Eye

Y. Geng[1A,1B], L. Schery[1A], K. Ahmad[1A], R.T. Libby[1A,1C], D.R. Williams[1A,1D]. [A]Center for Visual Science, [B]the Institute of Optics, [C]Flaum Eye Institute, [D]the Institute of Optics and Flaum Eye Institute, [1]University of Rochester, Rochester, NY.

Purpose: We have measured the wave aberration of the mouse eye to establish the requirements for an adaptive optics camera that could achieve diffraction-limited retinal imaging. Garcia de la Cera et al. [1] reported aberration measurements up to 4th order on 12 mouse eyes. We extend these data by measuring a larger number of aberrations across a larger, fully dilated pupil.
Methods: Using a Shack-Hartmann wavefront sensor operating in reflected light (794 nm), we measured aberrations up to 10th order with 321 lenslets filling a 2 mm, dilated pupil. C57BL/6J pigmented (n=5) and albino mice (n=2) between 75 and 150 days of age were used. Each was anesthetized and aligned so that the first Purkinje image of a source on the optical axis of the instrument was centered in the mouse's pupil. Speckle was reduced by scanning the beam across the retina. Eyes were periodically lubricated to avoid corneal dehydration.
Results: As reported by Biss et al. [2] and Garcia de la Cera et al. [1], wavefront sensor spot quality was poor in mice compared with primates. Pigmented mice had better spot quality than albino mice. Nonetheless, we obtained repeatable wave aberration measurements. At the same numerical aperture, the higher order aberrations of the mouse eye are smaller than those of the human eye. Moreover, the numerical aperture of the mouse eye can be twice as large as that of the human, making it theoretically possible to achieve a resolution of 0.7 um at 550 nm, two times better than can be achieved in human. An adaptive optics camera for the mouse would need to measure and correct Zernike orders up to and including at least 6th order to achieve diffraction-limited imaging (Strehl ratio > 0.8).
Conclusions: The ability to capture the entire wave aberration in the mouse eye over a fully dilated pupil with reflected light is promising for high-speed adaptive correction of mouse retinal images. Such an instrument could allow microscopic imaging of retinal development, disease progression, or the efficacy of therapy in single animals over time.
References: [1] Garcia de la Cera E, Rodriguez G, Llorente L, Schaeffel F, Marcos S. Optical aberrations in the mouse eye. *Vision Res*. 2006;46:2546-2553. [2] Biss DP, Sumorok D, Burns SA, *et al*. In vivo fluorescent imaging of the mouse retina using adaptive optics. *Opt Lett*. 2007;32:659-661.
CR: Y. Geng, None; **L. Schery**, None; **K. Ahmad**, None; **R.T. Libby**, None; **D.R. Williams**, Optos, C; #6,199,986, #6,299,311, #6,827,444, #6,264,328, #6,338,559, P; U.S. Patents #5,777,719, #5,949,521, #6,095,651, #6,379,005, #6,948,818, P.
Support: NIH Grant EY 001319, EY014375; NSF STC grant No. AST-9876783; Research to Prevent Blindness.

3961 - A183
Variability in the Optical Quality Within a Single Strain of Pigmented Rats

M. Bird[1A], M.C.W. Campbell[1B,2], M.L. Kisilak[1B], K. Bunghardt[1A], N.J. Gibson[1C], E.L. Irving[1D]. [A]Physics & Astronomy, [B]Physics & Astronomy/School of Optometry, [C]School of Optometry/Department of Psychology, [D]School of Optometry, [1]University of Waterloo, Waterloo, ON, Canada; [2]Guelph Waterloo Physics Institute, Waterloo, ON, Canada.

Purpose: Campbell and Hughes (1981) published a rat schematic eye showing overcorrected spherical aberration (SA), in agreement with measurements on pigmented DA rats. In this case, the optical power decrease in the periphery of the gradient refractive index lens is not completly balanced by the power increase in the peripheral cornea. More recently, we showed that the total root mean square (RMS) higher-order aberrations (HOA) of Long Evans rats within 20 degrees of the optical axis agreed with the model's predictions. However, we have also shown variability in refraction among rat strains used as models of disease and others have reported variability in the sign of SA. Here we investigate SA in pigmented, Long Evans rats experimentally and by modeling.
Methods: Hartmann-Shack (H-S) measurements were acquired from the eyes of Long Evans rats, either awake or under sedation with natural or dilated pupils. SA was assessed with retinoscopy in 2 additional animals. The relative speed of the retinoscopic reflex in the pupil centre and periphery was assessed. A Zemax model of the rat eye, including a gradient refractive index lens, was used to assess the sensitivity of SA of the eye to corneal shape.
Results: For many measurements, the H-S patterns could not be analysed due to poor tear film and optical quality issues. All Long Evans rats were hyperopic, in agreement with the published eye model. The average Zernike coefficient for SA across 7 eyes at a 1.47 mm pupil was 0.04 waves, ranging from -0.007 waves (overcorrected) to 0.1 waves (undercorrected). Pupil sizes of 1.88 mm (5 eyes) and 2.3 mm (3 eyes) gave average SA values of 0.018 waves and -0.01 waves respectively. Retinoscopy reflexes were consistent with undercorrected SA in the 4 eyes measured. For the corneal asphericity measured for DA rats (-0.14), the model predicted an overcorrected SA of -0.02 waves (1.47 mm pupil), -0.05 waves (1.88 mm) and -0.12 waves (2.3 mm pupil). However, reducing the corneal asphericity in the model reduced SA progressively. It changed to undercorrected SA at a corneal asphericity of 0.06.
Conclusions: Eyes within a single strain of pigmented rats exhibit SA of differing sign. Although the schematic eye correctly predicts the RMS HOA of Long Evans rats, it does not predict the average SA. Our analysis shows that SA is sensitive to the asphericity of the rat cornea. Variability in refraction and SA needs to be taken into account when designing contact lenses and imaging the fundus of the rat, an important animal model of disease.
CR: M. Bird, None; **M.C.W. Campbell**, None; **M.L. Kisilak**, None; **K. Bunghardt**, None; **N.J. Gibson**, None; **E.L. Irving**, None.
Support: NSERC, CFI, CIPI, CRC

3962 - A184
Wavefront Aberrations and Modulation Transfer Functions of Multifocal Intraocular Lenses in Visible and Infrared Wavelengths

Y. Hirohara[1,2], M. Saika[1], T. Fujikado[2], T. Oshika[3], T. Mihashi[1,2]. [1]Optics Laboratory, Topcon Corporation, Itabashi, Japan; [2]Department of Applied Visual Science, Osaka University Graduate School of Medicine, Suita, Japan; [3]Dept of Ophthalmology, Institute of Clin, University of Tsukuba, Tsukuba, Japan.

Purpose: We measured three types of IOLs using a two-wavelength Shack-Hartmann wavefront aberrometer (SHWA) and modulation transfer function (MTF) equipment and investigated the validity of a wavefront aberration (WA) measurement of multifocal IOLs.
Methods: A monofocal IOL (Sensar AR40e AMO), a refractive multifocal IOL (ReZoom NXG1 AMO), and an apodized diffractive multifocal IOL (AcrySof Restor SA60D3 Alcon) were measured. We developed an aberration-free artificial eye (AFAE) which could hold an IOL to measure its aberration and MTF in the water. Wavefront sensing (WS) was performed on the AFAE with each IOL using a two-wavelength (561nm and 840nm) SHWA. Through focus MTF (TF-MTF) of the AFAE with the IOLs were also measured using a TF-MTF measurement system (MATRIX PLUS Nanotex corp.) in visible and near infrared (NIR) wavelengths.
Results: RMS of the WAs of the AR40e was 0.01μm for the 4-mm circle area and 0.06μm for the 6-mm circular area. Spatial pattern of Hartmann image of the NXG1 was distorted and the distortion was rotationally symmetrical because the IOL had five annular power zones. TF-MTF calculated from the WAs had peaks at two defocus positions. PSFs in the Hartmann image of the AFAE with SA60D3 were blurred a little with 840-nm WS but some PSFs were split into two spots with 561-nm WS. We could calculate distant or near refraction selecting one of those split PSFs. TF-MTF of the AR40e had a peak only at one focus position, but that of NXG1 had peaks at two defocus positions in both wavelengths. TF-MTF of the SA60D3 had peaks at two defocus positions in 561nm, but one peak in 840nm.
Conclusions: We could evaluate multifocality of the diffractive multifocal IOL using the visible wavelength. We also confirmed that wavefront sensing of a diffractive multifocal IOL with an infrared wavelength is valid to measure distance vision.
CR: Y. Hirohara, Topcon Corp., E; **M. Saika**, Topcon Corp., E; **T. Fujikado**, None; **T. Oshika**, None; **T. Mihashi**, Topcon Corp., E.
Support: None

3963 - A185
Comparison Between Simulated and Measured Subjective Depth of Focus in Presence of Various Monochromatic Aberrations

R. Legras, Y. Benard. Laboratoire aimé Cotton, CNRS, Université Paris Sud, Orsay, France.

Purpose: The two objectives were to measure the impact of spherical aberration (SA) and vertical coma on subjective depth-of-focus (DoF) and to examine the accuracy of simulated images, calculated from a numerical eye model, in predicting those impacts.
Methods: Subjective DoF was defined as the range of defocus for which the target was still perceived acceptable (objectionable blur), and was measured on two letter sizes (i.e. three high contrast letters of 20/50 or 20/25). We used an adaptive optics system to dynamically control the observer's wavefront aberration and accommodation. The subject's head was stabilized with a bite bar. The subjective DoF was measured with a 0.18-D step using two procedures. In the first one, the subject changed the defocus by reshaping the mirror, when viewing the original letters (i.e. unaberrated target). In the second procedure, the subject changed displayed images, which were calculated for various defocus, using a numerical eye model. We measured the DoF of 4 non-presbyopic subjects corrected for their entire eye aberrations (i) with a 6-mm and (ii) a 3-mm pupil size, (iii) and (iv) with the addition of 0.3-μm and 0.6-μm of positive SA, (v) and (vi) with the addition of 0.3-μm and 0.6-μm of vertical coma. Conditions (iii) to (vi) were measured with a 6-mm pupil size.
Results: Using the 20/50 letter size, we obtained a mean DoF of 1.35-D for the naked eye with a 6-mm pupil size. Subjective DoF increased by 25, 45, 53, and 60% with the addition of respectively 0.3-μm of coma and SA, and 0.6-μm of SA and coma. Using the 20/25 letter size, compared to the naked eye condition (1.10-D), DoF increased by 6, 15, 14 and 19%. DoF measured on simulated images calculated from a numerical eye model were comparable to DoF measured using the mirror, whatever the condition and letter size (r^2 = 0.79 and 0.71 for the 20/50 and 20/25 letter sizes respectively). rMTF- or rOTF-based image quality metrics were not able to predict subjective DoF (r^2=0.24) or DoF measured with calculated images (r^2 = 0.24).
Conclusions: Vertical coma and SA increased subjective DoF. Subjective DoF could be predicted using simulated images.
CR: R. Legras, None; **Y. Benard**, None.
Support: None

3964 - A186
Optimization of Subjective Depth of Focus With Combinations of Spherical Aberration and Secondary Spherical Aberration

Y. Benard, R. Legras. Laboratoire Aimé Cotton, CNRS, Université Paris Sud, Orsay, France.

Purpose: To optimize the subjective depth of focus (DoF) by introducing combinations of spherical aberration (SA) and secondary SA.
Methods: We measured subjective DoF for various aberration conditions at 3 pupil sizes (i.e. 3, 4.5, and 6-mm) using through-focus simulated images calculated from a numerical eye model. We dynamically controlled the observer's wavefront aberration and accommodation with an adaptive optics system. Subjective DoF was defined as the range of defocus for which the target was still perceived acceptable (objectionable blur). The subject viewed the target through an artificial pupil conjugated to the pupil plane and changed the defocus term in a 0.18-D step by changing the displayed images which were calculated for various defocus. We measured the subjective DoF on 3 non-presbyopic subjects, while fully correcting their aberrations. We displayed images calculated with various levels of SA (i.e. -0.6-μm, -0.3-μm, 0-μm, +0.3-μm, +0.6-μm), secondary SA (i.e. -0.3-μm, -0.15-μm, 0-μm, +0.15-μm, +0.3-μm) and combinations of SA and secondary SA (i.e. 25 combinations of aberrations).
Results: We found a mean subjective DoF of 1.97-D with a 3-mm pupil size, which decreased by 34% with a 6-mm pupil diameter and by 28% with a 4.5-mm pupil. Two distinct DoF separated by 0.14-D to 1.26-D were sometimes observed with combinations of SA and secondary SA of opposite signs. However, considering the DoF as the range between the two extreme limits, we observed with the 6-mm pupil size, an increase of subjective DoF of 45% and 64% with the addition of 0.3 and 0.6-μm of SA (i.e. positive and negative averaged), and of 52% and 117% with the addition of 0.15 and 0.3-μm of secondary SA. The combinations of SA and secondary SA that most increased the DoF are the one with opposite signs: a DoF up to three and a half times larger (i.e. 4.78-D) than the naked eye. Reducing the pupil size minimized the effect of aberrations on subjective DoF.
Conclusions: The sign of SA or secondary SA is not important as long as they are introduced in opposite signs. Subjective DoF was multiplied by 3.6 with 0.6-μm of SA and 0.3-μm of secondary SA of opposite signs, but with a range of unacceptable vision in it.
CR: Y. Benard, None; **R. Legras**, None.
Support: None

3965 - A187
Impact of Higher Order Aberrations on Objective Depth of Focus in Pseudophakic Patients

Y. Nochez[1], M. Censier[1], A. Cardon[1], S. Majzoub[1], P.-J. Pisella[2]. [1]Ophthalmology, Bretonneau Hospital of Tours, Tours, France; [2]Ophthalmology, University Hospital of Tours, Tours, France.

Purpose: To determine the role of corneal and internal higher order aberrations on objective depth-of-focus in pseudophakic patients. To assess respective contribution of aberrations to pseudo-accommodation in pseudophakic patients with monofocal aspheric IOLs.
Methods: This study included 60 eyes (40 patients) that received an aspherical IOL (AcriSmart 36A® or AcriSmart 46LC® or Quatrix®) after a micro-incision cataract surgery. 6 months postoperatively, total and corneal aberrations for a standardized pupil size of 6 mm were computed using Wavescan Aberrometer (AMO, USA) and Atlas® topographer (Carl Zeiss Meditec, USA). Depth of focus (DOF) and degree of apparent accommodation were obtained when the defocused visual acuity becomes half of the best corrected visual acuity (BCVA) with MTF measurements (defined as the range of defocus in which MTF is greater than 80% of maximal MTF) using the Objective Quality Analysis System® (Visiometrics, Spain).
Results: Results demonstrated that DOF appeared to be strongly correlated with SA (r2=0,52 with p=0,002) and with trefoil (r2=0,53 with p=0,001). However, DOF was not correlated with coma values (r2 = 0,002 with p=0,87). Influence of refractive astigmatism will be also presented.
Conclusions: Higher order aberrations should be measured preoperatively. Indeed, high level of corneal trefoil may be advantageous for DOF even if we reduced total residual SA close to zero. The relationship of all HOA on image quality and DOF has to be considered.
CR: Y. nochez, None; **M. Censier**, None; **A. Cardon**, None; **S. Majzoub**, None; **P.-J. Pisella**, None.
Support: None

3966 - A188
Relationship Between Visual Acuity, Pupil Size and Refractive Difference in Pseudophakic Monovision

T. Kawamorita[1], H. Uozato[1], N. Nakayama[2], M. Shindo[2], T. Hannda[1], M. Ito[1], K. Shimizu[3]. [1]Orthoptics and Visual Science, Kitasato University School, Sagamihara-shi, Japan; [2]Ophthalmology and Visual Science, Kitasato University Graduate School, Sagamihara-shi, Japan; [3]Ophthalmology, Kitasato University School of Medicine, Sagamihara-shi, Japan.

Purpose: To investigate the relationship between pupil size and estimated visual acuity in pseudophakic monovision with ray tracing.
Methods: For the simulation, a modified Liou-Brennan model eye was used. The model eye was designed to include a centered optical system, corneal asphericity, a pupil, a Stiles-Crawford effect, an intraocular lens, and chromatic aberration. Calculation of the modulation transfer function (MTF) was performed with ZEMAX software. Visual acuity was estimated from the MTF and the retinal threshold curve. The sizes of the entrance pupil were 2.0, 2.5, 3.0, and 4.0 mm.
Results: Decreasing pupil diameter and increasing myopia progressively improved near visual acuity. For an entrance pupil size of 2.5-mm and a refractive difference of 1.5 D, the estimated visual acuities were 0.1 logMAR or better from far to a distance of 40 cm, and the estimated logMAR value (Snellen; metric) in the non-dominant eye at 40 cm was 0.06 (20/23; 6/6.9).
Conclusions: Our results would be of use to help predict visual acuity when using the pseudophakic monovision technique and to determine the optimum refractive difference from pupil size. Also, in cases of patients with a pupil size less 2.5 mm, a 1.5 D interocular difference in refractive error is effective for patients who have a near visual acuity of approximately 0.1 logMAR and excellent intermediate visual acuity.
CR: T. Kawamorita, None; **H. Uozato**, None; **N. Nakayama**, None; **M. Shindo**, None; **T. Hannda**, None; **M. Ito**, None; **K. Shimizu**, None.
Support: a grant from Kitasato University School of Allied Health Sciences (Grant-in-Aid for Research Project, No. 2009-6558) (T. K.)

3967 - A189
Cut-Off Values in Root Mean Square(rms) of Ocular Higher-Order Aberrations for Differentiating Normal Eyes From Pathological Conditions

M. Saika[1,2A], T. Nakagawa[2B], Y. Kitaguchi[2A], Y. Hirohara[1,2A], T. Mihashi[1,2A], N. Maeda[2B], T. Fujikado[2A]. [1]Optics Lab, Topcon Corp, Itabashi, Japan; [A]Applied visual science, [B]Department of Ophthalmology, [2]Osaka University Medical School, Suita, Japan.

Purpose: To define the cut-off values of wavefront aberrations by comparing in normal eyes with keratoconic suspect, LASIK, or cataractous eyes.
Methods: Wavefront sensing was performed in 65 normal eyes (N), 46 keratoconic suspect eyes (KCS), 50 LASIK eyes (L) and 111 cataractous eyes (CAT) with a Shack-Hartmann aberrometer (KR-9000PW, Topcon). The ocular wavefront aberrations were analyzed with normalized Zernike polynomials up to 4th order for 4-mm diameter circular area and with normalized Zernike polynomials up to 6th order for 6-mm. Means and standard deviations (SD) were calculated with RMS of total high-order aberrations (TH-RMS). In each category, the receiver operating characteristic (ROC) between normal and the category was analyzed. Cut-off values of the RMS were determined with both sensitivity and the specificity.
Results: TH-RMSs for each category were 0.09±0.03(mean±SD) μm (N), 0.36±0.26 μm (KCS), 0.19±0.07μm (L), and 0.27±0.14μm (CAT) for 4-mm diameter, and 0.30±0.11 μm (N), 1.05±0.65 μm (KCS), 0.74±0.24 μm (L), and 0.74±0.33 μm (CAT) for 6-mm diameter. The mean of TH-RMS for the normal eye was in agreement with previous studies(Howland, 2002). The ROC analysis showed the cut-off values of N to KCS, to L, and to CAT with 4mm TH-RMS (area under ROC curve) were 0.13 μm (0.928), 0.13 μm (0.909), and 0.15 μm (0.957) respectively. The cut-off of 6mm TH-RMS were 0.43 μm (0.908), 0.49 μm (0.987), and 0.45 μm (0.954).
Conclusions: We determined the cut-off value from the average of three ROC results. The cut-off value of TH-RMS was 0.14 μm in 4-mm pupil and 0.46 μm in 6-mm pupil. If we suppose the distribution of TH-RMS of normal eyes is Gaussian , 95%(mean±1.96SD) of the normal eyes lie between 0.03 to 0.15 for 4-mm diameter and 0.08 to 0.52 for 6-mm diameter. This is consistent with the cut-off values we obtained in this study.
CR: M. Saika, topcon, E; **T. Nakagawa**, None; **Y. Kitaguchi**, None; **Y. Hirohara**, topcon, E; **T. Mihashi**, topcon, E; **N. Maeda**, None; **T. Fujikado**, None.
Support: None

3968 - A190
Wavefront Aberrations Due to a Gaussian Model of Foveal Edema

B. Tan, J.M. Wanek, M. Shahidi. Ophthalmology & Visual Sciences, Univ. of Illinois at Chicago, Chicago, IL.

Purpose: The presence of foveal edema can degrade the optical performance of the eye by introducing increased wavefront aberrations (WA). The purpose of this study was to simulate the type and level of WA caused by a convex vitreoretinal interface (CVRI) due to foveal edema.
Methods: A modified Navarro eye model was incorporated into a ZEMAX model of a Shack-Hartmann wavefront sensor. The CVRI was represented by a Gaussian function (σ=106 μm). The incoming rays were partially diffusively reflected and partially refracted by the VRI. The rays were focused on the photoreceptor layer and diffusively reflected. The outgoing rays were again refracted by the VRI before exiting the eye. WA were simulated as a function of the CVRI maximum peak height (250 to 400 μm from photoreceptor cell layer), eccentricity with respect to peak (0 to 350 μm), and retinal refractive index (1.36 to 1.47). Lower order aberrations (LOA) (2^{nd}) and higher order aberrations (HOA) (3^{rd} - 7^{th}) were represented by Zernike polynomials.
Results: The incident rays reflected from the VRI primarily introduced LOA of defocus which was maximum at the CVRI peak and decreased in the periphery. The outgoing rays refracted by the VRI generated both LOA and HOA. A 60% increase (250 to 400 μm) in the CVRI peak height resulted in 9 and 16 fold increases in LOA and HOA root mean square (RMS) errors, respectively. Symmetrical aberrations were largest at the CVRI peak and decreased in the periphery. Asymmetrical aberrations were negligible at the CVRI peak. Astigmatism, trefoil, and terafoil were largest at the eccentricity of 100 μm, while coma and 2nd order astigmatism were largest at the eccentricity of 67 μm. An 8% increase in the refractive index of the retina resulted in 6 and 8 fold increases in LOA and HOA RMS, respectively.
Conclusion: Symmetrical aberrations were primarily present at the CVRI peak, while asymmetrical aberrations were more pronounced in the periphery. The magnitude of aberrations was dependent on the peak height of the CVRI and refractive index of the retina. This model may be applied for estimating the type and level of aberrations in patients with foveal edema.
CR: B. Tan, None; **J.M. Wanek**, None; **M. Shahidi**, None.
Support: NEI, Dept of VA, RPB

3969 - A191
Spherical Aberration and Contrast Sensitivity After Custom Surgeries

J. Barreto, Jr., R. Garcia, M.V. Netto, S.J. Bechara, M.R. Alves. Department of Ophthalmology, University of Sao Paulo, Sao Paulo, Brazil.

Purpose: To compare spherical aberration (SA) and contrast sensitivity after custom surgeries for myopia and myopic astigmatism correction.
Methods: Chart review of 70 eyes (35 patients) submitted to wavefront-guided LASIK (WFG-LASIK) and wavefront-guided PRK (WFG-PRK) with myopia up to 5D and astigmatism up to 1,5D. Wavefront analysis and contrast sensitivity were performed preoperatively and at one, three, six and twelve months postoperatively.
Results: The mean pre-treatment SA was 0,13±0.07μm in the WFG-LASIK group and 0,12±0.08μm in the WFG-PRK group (p = 0,344). In the WFG-LASIK group, the mean SA was 0,19±0,10μm (induction of 1,46) after 12 months postoperatively, and in the WFG-PRK group, 0,17±0,11 μm (induction of 1,41) (p = 0,089). Photopic contrast sensitivity improved significantly for most frequencies for both techniques. No significant improvement was found for most mesopic contrast sensitivity frequencies for both groups.
Conclusions: Despite SA induction, photopic contrast sensitivity has improved after WFG-LASIK and WFG-PRK without significant difference between them. Changes in low levels of SA RMS wavefront error poorly predict visual performance.
CR: J. Barreto, Jr., None; **R. Garcia**, None; **M.V. Netto**, None; **S.J. Bechara**, None; **M.R. Alves**, None.
Support: FAPESP (07/50516-2)

3970 - A192
Visual Performance With Scratched Antireflective Coated Spectacle Lenses

G.A. Zikos[1A], R. Robilotto[2], A. Selenow[1B], S.R. Ali[1C]. [A]Institute for Vision Research, [B]Inst Vision Research, [C]Inst of Vision Research, [1]Manhattan Vision Associates, New York, NY; [2]Institute for Vision Research, Manhattan Vision Associates, Tarrytown, NY.

Purpose: To compare the visual performance of scratched CR39 spectacle lenses with different antireflective (AR) coatings.
Methods: : 20 subjects (mean age=28y) were tested monocularly while wearing two different plano CR39 lenses. The tested lenses were AR coated with either: (A) Crizal Avancé with Scotchgard Protector or (B) leading competitor AR. All the lenses used were subjected to the same Bayer abrasion test before use. The mean scores were 12 for lens A and 5 for lens B. The subjects were either emmetropic or corrected with contact lenses. Visual performance was tested in the presence of glare in an environment simulating nighttime driving conditions, by measuring resolution thresholds of a tumbling "E" at 5 different contrast levels (~6% to ~100%) at a distance of 10M. Targets were presented by using a Cambridge Research Systems Ltd. ViSaGe on a SONY GDM-F20 CRT. A 4AFC linear staircase procedure was used.
Results: Significant improvements in visual performance were seen at all contrast levels tested. The mean differences were 0.04 LogMAR (about half a VA line) ($p<0.01$)

Contrast	LogMAR VA	
Level	Lens A	Lens B
1	0.11	0.15
0.5	0.17	0.20
0.25	0.27	0.33
0.13	0.42	0.46
0.06	0.57	0.6

Conclusions: The improved scratch resistance of the new AR coatings can provide significant visual benefits in visually challenging environments such as during night driving. There could be potential implications on safety when lenses get abraded after long periods of use.
CR: **G.A. Zikos**, Essilor, F; **R. Robilotto**, Essilor, F; **A. Selenow**, Essilor, F; **S.R. Ali**, Essilor, F.
Support: Essilor USA

3971 - A193
Optical Quality and Intraocular Scattering in Normal Young Human Population: Normalization Study

J. Ondategui-Parra[1], J. Martínez-Roda[1], F. Burgos[2], A. Giner[2], M. Vilaseca[2], J. Pujol[2]. [1]Technical University of Catalonia - University Vision Centre (CUV), Terrassa, Barcelona, Spain; [2]Technical University of Catalonia - Centre for Sensors, Instruments and Systems Development (CD6), Terrassa, Barcelona, Spain.

Purpose: To obtain normal values of the optical quality (OQ) of the eye and intraocular scattering (IS) in healthy young population. To calculate neural CSF (nCSF) from measured Modulation Transfer Function (MTF) and Contrast Sensitivity Function (CSF).
Methods: We evaluated the retinal image quality and CSF in 181 eyes within a group of 107 healthy young patients. Their best spectacle-corrected visual acuity (BSCVA) was 20/20 or better assessed with a standard logMAR chart. Retinal images were acquired with a clinical double-pass (DP) instrument (OQAS, Visiometrics, Spain) using a 4-mm exit pupil diameter. DP images contain information about aberrations and IS (*Diaz-Douton et al. IOVS 2006).* From the DP images, several parameters related with the OQ of the eye (MTF, Strehl ratio and OQAS values at contrasts 100%, 20% and 9%) and with the IS (Objective Scatter Index, OSI) were obtained. CSF was measured with a CSV-1000 test (Vector Vision, Greenville, OH) in mesopic conditions. We computed the nCSF of all patients from the corresponding CSF and MTF ratio.
Results: Mean age was 22.47 years ± 3.04 (SD) (range 19 to 30 yr.) and 43.92 % were men. Mean BSCVA was -0.14±0.07 log MAR. Normal OQ and IS parameters were (Mean ± SD): Strehl ratio 0.27±0.06; OQAS Value 100% 1.48±0.24; OQAS Value 20% 1.58±0.32; OQAS Value 9% 1.64±0.39 and OSI 0.38±0.19. The corresponding measured CSF were 1.63±0.20 for 3 cpd frequency, 1.78±0.21 (6 cpd), 1.4±0.26 (12 cpd), and 0.96±0.29 (18 cpd). nCSF calculated was 1.76±0.21 (3 cpd), 2.12±0.23 (6 cpd), 2.00±0.28 (12 cpd), and 1.86±0.33 (18 cpd). As expected, OQ results were similar to those found in other previous non-clinical studies. OSI values showed a low IS in the studied population.
Conclusions: We obtained normal values of OQ and IS in healthy young adult population with a DP system in a clinical environment. We calculated nCSF comparing MTF and CSF values. These results can be a referent for the early detection of pathologies where OQ, IS or sensory function are impaired. Future work is oriented to study OQ and IS in other age ranges.
CR: **J. Ondategui-Parra**, None; **J. Martínez-Roda**, None; **F. Burgos**, None; **A. Giner**, None; **M. Vilaseca**, None; **J. Pujol**, Visiometrics, P.
Support: "Ministerio de Educación y Ciencia", Spain (grant nº DPI2008-06455-C02-01); "Ministerio de Asuntos Exteriores y de Cooperación", Spain (grant nº D/017822/08), and Visiometrics.